Proof of concept of hydrothermal oxidation for treatment of triazine-based spent and unspent H2S scavengers from offshore oil and gas production

Montesantos, Nikos; Nikbakht Fini, Mahdi; Muff, Jens; Maschietti, Marco

Published in:
Chemical Engineering Journal

DOI (link to publication from Publisher):
10.1016/j.cej.2021.131020

Publication date:
2022

Document Version
Publisher's PDF, also known as Version of record

Chemical Engineering Journal 427 (2022) 131020

Contents lists available at ScienceDirect

Chemical Engineering Journal

journal homepage: www.elsevier.com/locate/cej

Proof of concept of hydrothermal oxidation for treatment of triazine-based spent and unspent H_2S scavengers from offshore oil and gas production

Nikolaos Montesantos, Mahdi Nikbakht Fini, Jens Muff, Marco Maschietti *

Department of Chemistry and Bioscience, Aalborg University, Niels Bohrs Vej 8A, Esbjerg 6700, Denmark

ARTICLE INFO

Keywords:
Spent scavengers
Wet oxidation
Wastewater
Triazine
Ethanolamine
Dithiazine

ABSTRACT

The feasibility of the hydrothermal oxidation of a wastewater derived from H_2S scavenging operations, carried out in a topside offshore oil and gas installation, was demonstrated. The feed characterization showed the presence of mainly unreacted triazine (unspent scavenger), monoethanolamine and dithiazine (spent scavengers). The spent and unspent scavengers (SUS) were subjected to hydrothermal oxidation in a batch reactor at approximately 200 °C (low temperature, LT) and 350 °C (high temperature, HT), using oxygen in excess. The experiments were performed for six reaction times at each temperature, in the range 3 to 360 min at LT and 1 to 120 min at HT. Diluted SUS (COD around 30 g/kg) was used as reactor feed. The three main compounds of the SUS were not found in any of the oxidation products, which means they are fast converted. COD reductions up to 84% and 98% were obtained at LT and HT, respectively. A rate equation of second order with respect to the COD was found suitable to represent the rate of disappearance of COD, with the rate constant at HT approximately 70 times higher than at LT. The extensive analysis carried out on the reaction products showed the presence of C1-C4 carboxylic acids, pyridines and pyrazines as intermediate oxidation products. A clear trend towards complete mineralization of organic nitrogen to ammonium, except for small amounts of nitrate at LT, and of organic sulfur towards sulfate, was observed.

1. Introduction

Hydrogen sulfide (H_2S) is an extremely toxic, flammable and corrosive chemical, which is contained in the fluid phases produced in oil and gas extraction. The concentration of H_2S must be reduced to very low levels for safeguarding structures from corrosion, for export product quality constraints, as well as for safety, health and environmental reasons. In particular, the concentration of H_2S in natural gas for sale is typically required to be below 4 ppm. In offshore oil and gas production, the abatement of H_2S in the produced fluids is often carried out by injecting chemicals, called H_2S scavengers, which convert H_2S into substantially less harmful species. The H_2S scavenging operation can be carried out both upstream of the primary gas-oil–water separation and in the natural gas stream downstream of the said separation [1].

1,3,5-hexahydrotriazines (simply called triazines in this context) are widely used as H_2S scavengers, with water-soluble types such as 1,3,5-tri-(2-hydroxyethyl)-hexahydro-*S*-triazine (HET) being the most common [2]. In the scavenging of natural gas streams, basic aqueous solutions of HET are injected and dispersed into the gas, leading to the absorption of H_2S and the consequent reaction with HET in the aqueous phase. In industrial practice, HET is typically injected in large excess of the stoichiometric requirement, as a conservative measure in order to ensure the complete conversion of H_2S [1]. The commonly accepted reaction scheme consists of two successive substitutions of sulfur to nitrogen in the triazine ring with the release of one molecule of monoethanolamine (MEA) at each step, as reported in Fig. 1 [3–5]. For this reason, this chemical is also known as MEA-triazine in oil and gas practice. HET, MEA and 5-(2-hydroxyethyl)hexahydro-1,3,5-dithiazine (DTZ) are observed in industrial samples of reaction products, whereas the intermediate product (3,5-bis-(2-hydroxyethyl)hexahydro-1,3,5-thiadiazine, TDZ) is typically not detected. Trithiolanes and tetrathiepanes have also been reported [1], together with amorphous polymeric dithiazine (apDTZ), which is an S-rich insoluble product derived from DTZ polymerization and typically observed in highly-spent scavenger samples [5].

Downstream of the H_2S scavenger injection point, the aqueous phase containing unreacted (unspent) triazine and the reaction products (spent scavengers) is separated from the gas, resulting in a characteristic

* Corresponding author.
E-mail address: marco@bio.aau.dk (M. Maschietti).

https://doi.org/10.1016/j.cej.2021.131020
Received 22 May 2021; Received in revised form 21 June 2021; Accepted 22 June 2021
Available online 26 June 2021

wastewater stream (spent and unspent scavengers, SUS). In spite of the relatively small size of this stream, in comparison to the total produced water in offshore oil and gas installations, its management is problematic due to the scaling and fouling potential caused by its alkaline pH and DTZ polymerization [2]. It is therefore not uncommon that the SUS wastewater is discharged untreated into the sea due to lack of viable alternatives. However, the discharge of this wastewater has sometimes been associated with environmental issues [1]. For example, even though the discharge is generally permitted under surveillance, according to OSPAR triazine-based H_2S scavengers are not included in the list of chemicals posing little or no risk to the environment (PLONOR) [6]. In addition, MEA is defined as "harmful to aquatic life with long lasting effects" by the European Chemicals Agency (ECHA) [7]. To our knowledge, specific information on the environmental profile of DTZ is not available. Overall, we deem highly relevant to assess the feasibility of treating the SUS wastewater in offshore installations prior to discharge, with the aim of reducing the environmental impact on the aquatic environment.

The high concentration of organics containing sulfur and nitrogen in this wastewater, together with the low space availability in offshore installations, points to hydrothermal oxidative processes as candidates. The hydrothermal oxidation (HTO) of wastewater streams is carried out by heating and pressurizing the wastewater, mixing it with compressed air (or oxygen) and feeding it to a high-pressure high temperature (HPHT) reactor. Applications are known both in the supercritical [8–10] and in the subcritical water range [11,12]. Even though the supercritical water oxidation (SCWO) process is particularly favorable due to high reaction rates, technical issues (e.g. corrosion, salt precipitation, reaction instability) have limited the industrial applications so far [9,10]. On the other hand, the application in the subcritical water range (150–320 °C), also known as Wet Oxidation (WO), has found more extensive application, with examples on municipal sludge as well as on hazardous wastewater [12].

The WO process is generally considered appropriate for wastewaters with chemical oxygen demand (COD) of 20–200 g/L, while it is often used to reduce the toxicity of wastewater prior to biological treatment [13]. Downstream of the HPHT reactor, the reaction products are cooled and decompressed. Incomplete oxidation intermediates are typically water-soluble, leaving the spent gas free of pollutants [14]. Depending on the nature of the wastewater and the design of the reactor, the WO process can attain complete conversion of organics containing sulfur and nitrogen to CO_2, H_2O, sulfates, ammonium/ammonia, nitrates, and nitrogen [15]. The thermal energy released by the oxidation reactions makes the process autothermal, when the COD value exceeds 12–15 g/L. Operations at higher pressure and temperature conditions are characterized by relatively high oxygen solubility in the aqueous phase (e.g. greater than 3 g/L) and higher reaction rates [11]. This allows attaining lower reactor volumes, which is particularly relevant in offshore applications due to the abovementioned space limitations.

Successful applications of oxidation of organic sulfides (R-S-R'), nitriles (-C≡N), thiocyanates (S-C≡N) and phenols were reported [14]. The process is applied industrially to treat complex aqueous feeds such as sewage sludge and spent caustic, which are characterized by nitrogen- and sulfur-containing pollutants. For example, typical values of COD reduction on spent caustic are in the range 70% to 80% for reaction time of 60 min at 260 °C [16], while COD reductions in the range 53% to 61% were observed on municipal sludge for the same reaction time for temperatures in the range 220 °C to 240 °C [17]. The organic pollutants that contain nitrogen or sulfur are typically oxidized to sulfates and nitrates, as well as ammonia and small carboxylic acids, which are less harmful from an environmental point of view [15]. Although the inorganic salts are typically considered final products of the oxidation, some carboxylic acids (e.g. acetic acid) are refractory intermediate reaction products and require severe oxidation conditions (e.g. greater than 320 °C) to fully oxidize to CO_2 and water [18]. The process was also applied at research level with promising results on specific nitrogen-containing compounds (e.g. quinoline) and on formaldehyde, the latter of which may occur as hydrolysis product of triazines. For example, total organic carbon (TOC) reductions of 70% at 280 °C and 76 bar, after more than one hour reaction time, and 38% at 220 °C, after 3 h, were reported for formaldehyde and quinoline, respectively [19,20]. Even though research works on WO of wastewaters containing organic pollutants with S,N heteroatoms are reported, to our knowledge no literature work is available on the application of WO on wastewaters generated in the H_2S scavenging process with triazine.

This work presents an investigation of the WO of a SUS wastewater, with the aim of providing a proof of concept of the WO process on this type of wastewater and of generating reaction kinetics data supporting the basic design of a hydrothermal reactor. The experimental activities were based on a real sample of SUS wastewater obtained from an offshore oil and gas installation in the North Sea, where the H_2S scavenging process is carried out at pressures and temperatures in the range 30 to 40 bar and 130 °C to 150 °C, respectively, under excess of HET. Fouling issues related to apDTZ are not reported regarding this installation. The work plan encompassed both low reaction severity (i.e., approximately 200 °C and 80 bar) and high reaction severity (i.e., approximately 350 °C, 230 bar), in order to evaluate the capability of the process in decreasing the COD of the wastewater and to quantitate the differences in the reaction rate. The experiments were carried out using pure oxygen as an oxidant, in excess of the stoichiometric requirement. A rate equation based on COD was developed. In addition, the reaction products were analyzed in order to identify and quantitate key reaction intermediates and end products.

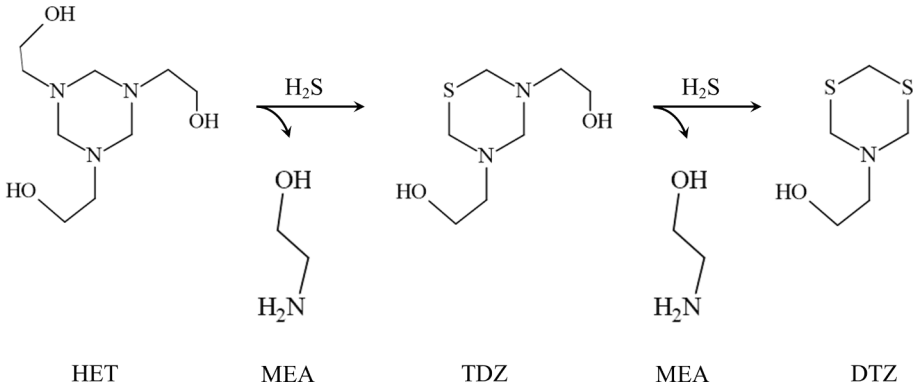

Fig. 1. H_2S scavenging reactions with 1,3,5-tri-(2-hydroxyethyl)-hexahydro-*S*-triazine (HET). MEA: Monoethanolamine; TDZ: 3,5-bis-(2-hydroxyethyl)hexahydro-1,3,5-thiadiazine; DTZ: 5-(2-hydroxyethyl)hexahydro-1,3,5-dithiazine.

2. Materials and methods

2.1. Materials

The SUS solution was retrieved from an offshore oil and gas processing installation in the North Sea. The sample was obtained downstream of two separators, the first one separating the gas from SUS and gas condensates, and the second one separating the gas condensates from the SUS. The sample was collected at atmospheric pressure and shipped to our laboratory where it was stored at 4 °C. Diethyl ether (DEE, ≥99%) and dichloromethane (DCM, ≥99.8%) from VWR were used as solvents for gas chromatography (GC). Dithiazine, (5-(2-hydroxyethyl)hexahydro-1,3,5-dithiazine, DTZ, $C_5H_{11}NOS_2$, CAS number 88891–55-8, ≥98%) from Toronto Research Chemicals, triazine (1,3,5-tri-(2-hydroxyethyl)-hexahydro-*S*-triazine, HET, $C_9H_{21}N_3O_3$, CAS number 4719–04-4, ≥95%) from Santa Cruz Biotechnology, monoethanolamine (MEA, C_2H_7NO, ≥99%) and pyridine (≥99%) from Acros were used as analytical standards. 1-Propanol (≥99.5%), 2-bromopyridine (≥99%), and methyl heptadecanoate (MHD, ≥99%) from VWR were used as internal standards for quantitative GC. Oxygen from a gas cylinder (O_2, ≥99.9%) from Air Liquide was used as oxidant for all experiments. A PlasmaCal standard from SCP Science was used for sulfur determination in aqueous samples. Potassium hydrogen phthalate (≥99.9, KHP) from VWR is used as standard for total carbon (TC), whereas sodium carbonate (≥99.9, Na_2CO_3) and sodium bicarbonate (≥99.9, $NaHCO_3$) from VWR are used as standards for total inorganic carbon (TIC) determinations and as eluents for ion chromatography (IC). Spectroquant cell test kits from Merck were used for quantitation of chemical oxygen demand (114540, 114541, 114555, 101797), total nitrogen (114763), and ammonium (114544). Acetic acid (≥99.7%) from VWR, formic (≥95%) and glycolic (≥99%) acid from Sigma-Aldrich and oxalic (≥99%), succinic (≥99.5%) and maleic (≥99%) acids from Merck were used as calibration standards for high-performance liquid chromatography (HPLC). Sulfuric acid (H_2SO_4, 98%) from VWR was used as eluent for HPLC.

2.2. Hydrothermal oxidation

The hydrothermal oxidation experiments were performed on a customized HPHT reactor (SITEC-Sieber Engineering AG, Switzerland) first described in a previous article [21]. The distinctive features of the HPHT setup consist in the possibility of: (i) injecting the feed to be subjected to hydrothermal treatment into the pre-heated pre-pressurized reaction chamber; (ii) controlling both the reaction temperature and pressure during the reaction; and (iii) quickly discharging and quenching the products. Some minor modifications of the apparatus were realized for this work, as shown in Fig. 2. The apparatus consists of a 99-mL high-pressure reactor vessel equipped with a heating jacket, automatic temperature control and manual pressure control via a hand pump.

In a typical oxidation experiment approximately 20 g of deionized water were precharged to the reactor vessel, which consequently was sealed. The reactor volume above the liquid was purged by opening the valve DV2 and gently flowing O_2 gas for 1–2 min through the TWV and V4 valves. After purging, V4 was closed, the reactor was pressurized with O_2 to approximately 35 bar, after which all valves were closed and the heating was turned on. The initial pressure was chosen to provide O_2 in excess of the stoichiometric requirement, obtained from the COD of the SUS to be loaded. The oxygen supply was around 190%-250% of the stoichiometric requirement of the SUS fed to the reactor. Mixing of the reactor contents was performed by an internal magnetic stirrer at approximately 25 revolutions per second (IKA C-MAG HS4). The oxidation of SUS was investigated at low temperature (LT, 200 °C ± 2 °C) and high temperature (HT, 346 °C ± 5 °C). The heating of the closed system up to the target temperature led the initial O_2 pressure of 35 bar to increase to 68 bar ± 2 bar and 205 bar ± 2 bar at LT and HT,

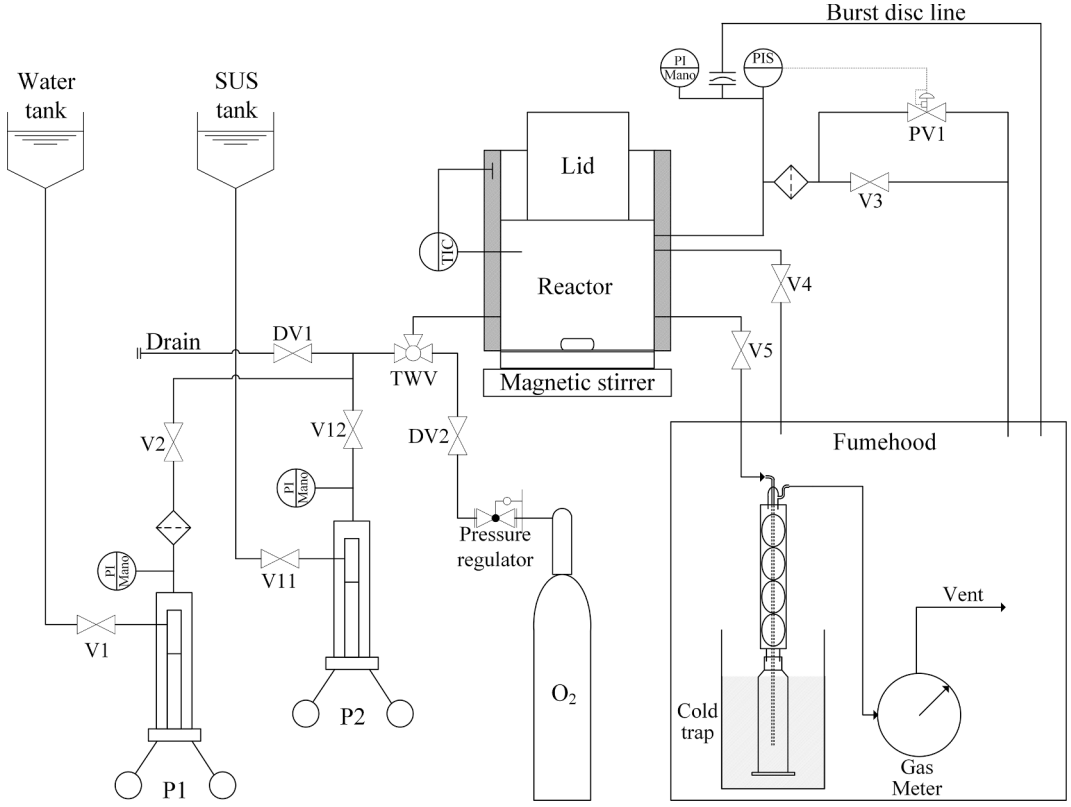

Fig. 2. Schematic diagram of the high-pressure high-temperature reactor system used in this work. V1-V12, DV1, DV2: On/Off valves; TWV: 3-way valve; P1: Hand pump for pressure regulation; P2: Hand pump for feed injection; PV1: Pneumatic safety valve.

respectively. When the desired reaction temperature was reached the SUS was injected by the high-pressure hand pump P2. Maintaining the SUS in the pump P2 during the reactor heating and pressurization allowed to keep the reactants at ambient temperature and avoid thermal decomposition before the injection into the reactor. The duration of the manual injection of the feed was in the range of 1.5 to 3.0 min. The reaction time is counted from the end of the injection in each experimental run (time $t = 0$). The injection of the room-temperature feed resulted in a modest temperature drop (10–20 °C), followed by a quick temperature increase after the end of the injection. The pressure increased during the injection, while it decreased to some extent for some time after the end of the injection. Examples of typical experimental P-T profiles are shown in Fig. 3, where the injection start and end, as well as the discharge times, are annotated. P-T profiles for all experimental conditions are available in the Supplementary Information. Pressure and temperature values associated with individual experimental runs were calculated as mean values:

$$f_{mean} = \frac{1}{t_r} \bullet \int_0^{t_r} f(t)dt$$

where f is either pressure or temperature, and t_r is the reaction time (from the end of the injection to the discharge).

When the desired reaction time was reached, the reactor contents were discharged through the valve V5 to a cold trap consisting of a condenser on top of a gas washing bottle. The washing bottle was submerged in ice and the condenser was cooled by tap water. The condensed liquid product in the cold trap was recovered, weighed and used for analytical characterization. The produced gases and unreacted oxygen were vented downstream of the cold trap.

2.3. Analytical characterization

The COD resulting from organic and inorganic components in the SUS and HTO samples was measured photometrically with the Spectroquant cell tests with different measurement ranges (i.e. 10–150 mg/L, 25–1500 mg/L, 0.5–10 g/L, 5–90 g/L). The COD of the SUS feed was measured at several different dilutions with a relative standard deviation (RSD) of 3%. The COD of the HTO products was always measured at two different dilution levels with an RSD always lower than 5%.

The total nitrogen (TN) measurement method transforms all organic and inorganic nitrogen to nitrate (EN ISO 11905–1) and consequently the nitrate is quantitated photometrically (DIN 38405–9). The ammonium cell test is calibrated to measure the concentration of nitrogen in the solution that corresponds to ammonium (NH_4^+) and ammonia (NH_3) by photometric determination (ISO 7150–1). The total nitrogen as well as the NH_4^+ concentrations were determined after dilution in duplicates with an RSD always lower than 3%.

The total organic carbon (TOC) of the aqueous samples was determined on an AnalytikJena multi N/C 2100S by thermocatalytic high-temperature digestion. For carbon determination, the produced CO_2 is measured by a nondispersive infrared sensor (NDIR). The instrument measures in parallel the TC and the TIC, while the TOC is calculated by difference. For the calibration, seven standards are used in the ranges 5–500 mg/L and 2.5–250 mg/L for TC and TIC, respectively. All measurements were performed in triplicate resulting in RSD values always lower than 1%. The instrument was always controlled with one of the standards prior to a series of measurements and was recalibrated in case the relative deviation between the measured and the theoretical value exceeded 10%.

Ion chromatography (IC) was performed on a Metrohm Vario system consisting of an 819 IC detector, 818 IC pump, 833 IC liquid handling system and 820 IC separation system with an anion exchange column (Metrosep A Supp 5–100/4.0). The eluents used were Na_2CO_3 (3.2 mM) and $NaHCO_3$ (1 mM) with a flow rate of 1 mL/min at 89 bar. Sulfate (SO_4^{2-}) and nitrate (NO_3^-) were quantitated over a calibration range of 2 – 10 mg/L. Nitrite (NO_2^-) was also calibrated but no peak was detected in any of the samples. The IC measurements were performed in duplicate resulting in an RSD always lower than 1%.

The total sulfur (TS) content was determined by Inductively Coupled Plasma - Optical Emission Spectrometry (ICP-OES) on a PerkinElmer Optima 8000 system [22,23]. Samples were prepared by acid digestion and dilution [24]. All dilutions were performed in de-ionized water using volumetric flasks (Class A) to match the calibration range of the PlasmaCAL standard (i.e. 0.2–20 mg/L). The R^2 of the calibration curve was always above 0.999 and the calibration was repeated after measuring one of the standards if the relative deviation between the theoretical value and the measurement exceeded 5%. The ICP samples were prepared by digesting 40 mL of SUS or reaction products, after dilution to match the calibration range, in an autoclave with 20 mL nitric acid aqueous solution (7 M) for 30 min at 120 °C and 2 bar. A blank of deionized water and nitric acid solution was digested as well for each collection of samples. The non-zero concentration for the blank was subtracted from the sample values to account for baseline errors. Duplicate samples were prepared for each reaction product, whereas the

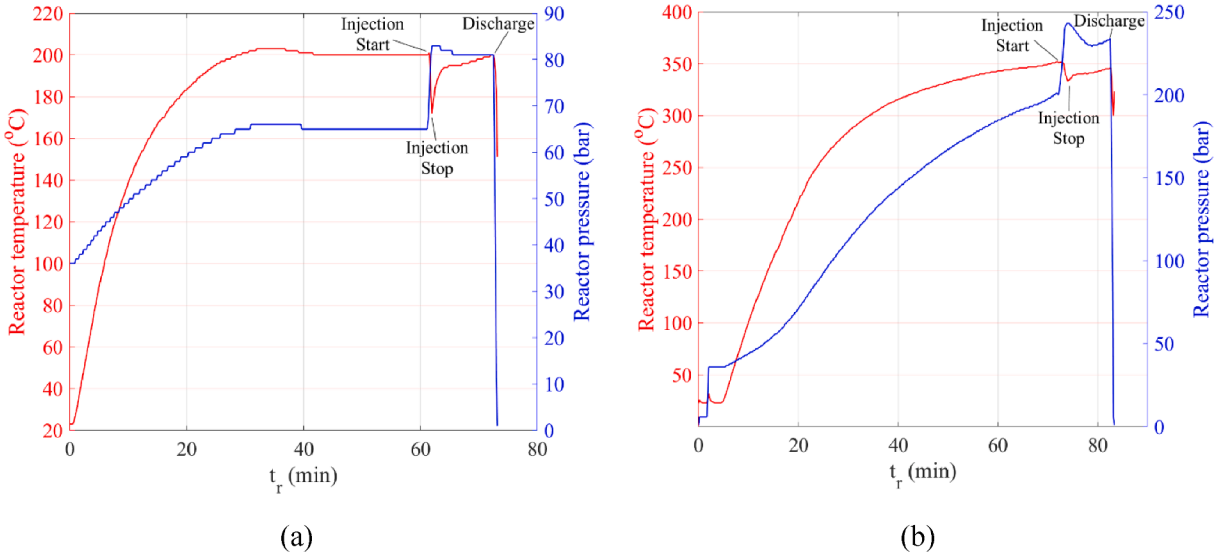

Fig. 3. Examples of pressure and temperature profiles for reactions at: (a) Low temperature and reaction time of 10 min; (b) High temperature and reaction time of 10 min.

analysis of the feed was repeated five times. Each sample was analyzed in triplicate by the ICP with RSD always lower than 2%.

Solid phase micro-extraction (SPME) GC–MS was performed for the qualitative characterization of the reaction products on a PerkinElmer Clarus 580 coupled with a Clarus SQ 8 S. 1 mL of each sample was heated in a screw-thread vial with septum cap to 60 °C and the SPME fiber (Polydimethylsiloxane/Divinylbenzene, Supelco 57346-U) was left in the headspace of the vial for 30 min. The GC program was: 50 °C initial temperature; 15 °C/min to 225 °C and hold for 10 min. The helium carrier gas was maintained at 1 mL/min, while the injector at 250 °C. The analytes were separated on a PerkinElmer Elite-5 column (30 m, 0.25 mm, 0.25 μm). The spectra corresponding to major chromatographic peaks were qualitatively compared with the NIST spectral database and a match factor above 700 was taken as a necessary condition for the assignment to a specific component.

Gas chromatography coupled with mass spectrometry (GC–MS) was used to quantitate DTZ in the SUS after a multistage liquid–liquid extraction procedure with DCM. Three consecutive extractions with solvent to feed ratio 20, 20 and 10 (mass basis) were performed to deplete DTZ from the aqueous phase. The yield of DTZ in the third stage was always lower than 5% of the total yield of DTZ, thus the selection of three extraction stages was deemed adequate. The analysis of the DCM-rich phase was performed on a PerkinElmer Clarus 680 GC coupled with a PerkinElmer Clarus SQ 8 T MS. The DTZ concentration was quantitated against an external standard calibration, using MHD as internal standard (IS) to account for inaccuracies between injections. The samples were always diluted in pure DCM to be in the range of the calibration standards (i.e. 0.2–1.0 g/L) and were spiked with the IS (0.5 g/L). The R^2 of the calibration curve was always $\geq$ 0.995. For all samples, 1 μL was injected in an Elite-5 column (30 m, 0.25 mm ID, 0.1 μm). The initial temperature of the oven was 120 °C and the temperature was ramped at 25 °C/min to 175 °C and consequently at 45 °C/min to 225 °C where it was held for 3 min. The injector temperature was maintained at 300 °C and the flow rate of the helium carrier gas at 1.0 mL/min. The concentration of DTZ was determined by calculating the relative response factor (RRF) of DTZ with respect to the IS in the standard solutions as: $(C_{DTZ}/C_{IS}) = RRF \bullet (A_{DTZ}/A_{IS})$ where C_{DTZ} and C_{IS} are the concentrations and A_{DTZ} and A_{IS} are the chromatographic areas of DTZ and IS, respectively. The mass of DTZ in the DCM-extract was then calculated using the density of pure DCM at ambient temperature, which allowed to calculate the mass fraction of DTZ in the SUS feed. Triplicate injections were performed, with the RSD always lower than 5% of the average measured value.

The same GC–MS system was used to quantitate a selection of components (e.g. pyridine) in the reaction products that appeared consistently in the qualitative SPME analysis. In this case the samples were extracted with DEE, with a solvent to feed ratio of 2 (mass basis), as this solvent was reported in the literature to be appropriate for extraction of pyridines from aqueous solutions [25]. The solvent extraction procedure was tested using a synthetic aqueous solution of pyridine (0.2 wt%). An extraction yield of pyridine of 85% ± 2% (average of two determinations) in a single extraction step was obtained and deemed acceptable. The GC program was: 40 °C initial temperature; 10 °C/min to 150 °C; 15 °C/min to 250 °C and hold for 3 min. An external standard calibration was performed using solutions of pyridine in DEE in the range 0.5–1.5 g/L including 2-bromopyridine as the IS (0.12 g/L). The RRF of pyridine was estimated in the same way as with the case of DTZ and was used to quantify the concentration of pyridine, pyrazine and a number of their alkyl derivatives. Consequently, the mass fractions were calculated by using the density of pure DEE at ambient temperature.

The concentration of HET and MEA was determined on a PerkinElmer Clarus 690 gas chromatograph equipped with a flame ionization detector (GC-FID). The quantitation was performed by an external calibration with five standards in the range of 1.0–7.5 g/L for HET and 0.50–3.75 g/L for MEA. Aqueous samples were diluted with deionized water to achieve concentrations within the abovementioned ranges and were spiked with a known amount of 1-propanol as an internal standard (1.2 g/L). For all samples 1 μL was injected in a PerkinElmer Elite5-Amine column (30 m, 0.32 mm, 1 μm). The injector was maintained at 200 °C and a split ratio of 50:1. The oven temperature was programmed as follows: initial temperature 75 °C maintained for 1 min; ramp 15 °C/min to 120 °C; ramp 40 °C/min to 200 °C; hold for 5 min. The FID detector was maintained at 300 °C. The concentrations of HET and MEA were calculated by estimating their RRF in the same manner as for the GC–MS quantitation of DTZ. Similarly, the mass fraction was calculated using the density of SUS.

The extraction and GC–MS analyses for DTZ as well as the GC-FID analyses for HET and MEA were performed for five samples of reaction products obtained for reaction times in the range 3 to 10 min at LT and 1 to 3 min at HT, which is to say the shortest reaction times at the two conditions (see Section 3). Since no DTZ, HET or MEA chromatographic peaks were observed in any of the analyzed samples, it was concluded that these components rapidly decompose.

The presence of small carboxylic acids (i.e. formic, acetic, succinic, glycolic, oxalic and maleic acid) as intermediate oxidation products was confirmed against analytical standards by HPLC on an Agilent HPLC 1260 Infinity with UV detector at 210 nm wavelength. Quantitative data are only reported for formic, acetic and succinic acid because the mass fractions of glycolic, oxalic and maleic acid were very low (i.e. $<$ 0.001 g/kg). The analytical procedure was inspired by a previous work [26]. The separation was performed at 25 °C in an Aminex HPX-87H column (ID: 7.8 mm; length: 300 mm; Particle size: 9 μm) from BIO-RAD. The eluent was a 0.005 M H_2SO_4 with a constant flow rate of 0.6 mL/min. The quantitation was performed by an external calibration of five levels for all identified carboxylic acids. Duplicate determinations were performed with an average RSD of 6%.

In addition to the chemical characterization, the density of the SUS feed and the reaction products was measured at 23 °C on an AntonParr DMA 35 EX.

3. Results and discussion

3.1. Characterization of the spent/unspent scavenger feed

The spent/unspent scavenger (SUS) feed solution appeared as a yellow liquid with a pungent sulfur smell (Fig. 4a). Solid precipitate, which may have suggested the presence of apDTZ, was neither observed in the sample as received nor after long storage time. It was observed that SUS samples left for a few weeks at ambient conditions exhibited a color change towards amber, while the same did not happen on the refrigerated samples stored at 4 °C. When received and after long gravity separation a thin hydrocarbon rich phase was observed on the top of the bulk aqueous solution, probably originating from gas condensate carryover. The separated hydrocarbon phase was very small compared to the bulk aqueous phase (i.e. $<$ 0.1 g/L). All oxidation experiments and analytical characterization were performed on the aqueous phase.

The physical and chemical properties of the SUS are reported in Table 1. As can be seen, the TOC and COD of the feed were quantitated to 64 g/kg and 241 g/kg, respectively, while the inorganic carbon (TIC) was quantitated to 2 g/kg, which means that almost all the carbon in the SUS is organic. The unreacted HET, MEA and the H_2S scavenging reaction product DTZ were quantitated to 85 g/kg, 38 g/kg and 31 g/kg, respectively. The carbon corresponding to HET, MEA and DTZ is approximately 68 g/kg, which is in fair agreement with the TOC value. The total nitrogen was quantitated to 32 g/kg and the total sulfur to 16 g/kg, while the nitrogen and sulfur corresponding to HET, MEA and DTZ are 28 g/kg and 12 g/kg. The mass balances of C, N and S indicate that these three species are the largely predominant solutes from a quantitative standpoint, with other organics present only in very small amount.

The SPME qualitative analysis of the SUS allowed identifying some additional organic components that are present in the SUS solution, all

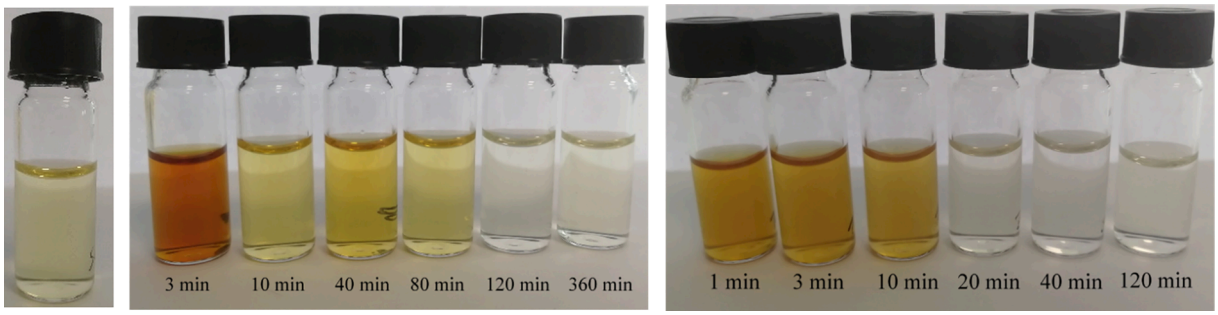

Fig. 4. (a) Spent/unspent scavengers; (b) Reaction products at low temperature; (c) Reaction products at high temperature. Corresponding reaction times are indicated.

Table 1
Physical and chemical properties of spent/unspent scavengers (SUS).

COD (g/kg)	241 ± 7	HET (g/kg)	85 ± 3
TOC (g/kg)	64 ± 6	MEA (g/kg)	38 ± 6
TIC (g/kg)	2 ± 0.1	DTZ (g/kg)	31 ± 1
TN (g/kg)	32 ± 2	Density at 23 °C (kg/m^3)	1042 ± 1
TS (g/kg)	16 ± 0.1	pH	8.9

of which contain either nitrogen or sulfur. One of the major chromatographic peaks was identified as 1,2,4-trithiolane. This species can be formed by reacting formaldehyde and bisulfide in aqueous phase [27] and formaldehyde can be produced by hydrolysis of HET [28], which provides a possible explanation for the presence of 1,2,4-trithiolane in the SUS. Other minor peaks included mainly single ring aromatic components (e.g. toluene and xylene) as well as a few naphthalene derivatives, probably originating from gas condensate.

3.2. Effect of reaction conditions on COD reduction

A total of eighteen oxidation experiments were performed. The parameters that were controlled for the experiments were the reaction time (t_r), the reaction temperature (T), and the oxygen supply which is expressed as a percentage of the stoichiometric oxygen requirement. The experiments were carried out at two temperature levels (i.e. LT and HT). Six reaction times were tested for each reaction temperature. The experiments at 40 min and 360 min at low temperature and at 10 min at high temperature were performed in triplicate to assess the reproducibility of the experimental procedure. The O_2 supply was always in excess than the stoichiometric requirement, with values ranging from 194% to 252%. The SUS feed was diluted approximately 1:5 (mass basis) with deionized water prior to each experiment. Considering the predilution as well as the further dilution in the reactor due to the precharged water (see Section 2.2), the resulting COD (indicated as COD_0) could be calculated and is reported in Table 2, together with t_r, T, P and the oxygen supply. In addition, the initial total organic carbon (TOC_0), total inorganic carbon (TIC_0), total nitrogen (TN_0) and total sulfur (TS_0) are reported, calculated taking into account the dilutions as explained above for COD_0.

The appearance of the reaction products can be observed in Fig. 4b and 4c for the low temperature and high temperature experiments, respectively. The products from the reactions up to 10 min had a darker color than the feed, while for higher reaction times the samples were transparent. With regard to the LT conditions, the pH of the reaction products was close to the pH of the feed (pH 8.9) for reaction times up to 3 min, while it was lower after 10 min (pH 6.4) and increased again up to pH 7.2–7.8 for longer reaction times (i.e. 40 to 360 min). All the reaction products at HT conditions exhibited pH values in the range of 8.2 to 8.6.

Fig. 5 shows the trend of the COD reduction as a function of the reaction time for the low temperature and high temperature oxidation experiments. The markers are the experimental values while the

Table 2
Experimental conditions for the hydrothermal oxidation reactions. t_r: reaction time; T: mean reaction temperature; P: mean reaction pressure; O_2: oxygen supply expressed as percentage of the stoichiometric requirement; COD_0, TOC_0, TIC_0 TN_0, TS_0: chemical oxygen demand, total organic carbon, total inorganic carbon, total nitrogen and total sulfur of the diluted feed.

t_r	T	P	O_2 supply	COD_0	TOC_0	TIC_0	TN_0	TS_0
(min)	(°C)	(bar)	(%)	(g/kg)				
Low temperature								
3	196	93	209	31	8.3	0.26	4.1	2.0
10	202	79	211	30	8.1	0.26	4.0	2.0
40	200	80	222	30	8.0	0.25	3.9	2.0
40	200	71	236	29	7.8	0.25	3.8	1.9
42	200	79	212	31	8.2	0.26	4.0	2.0
80	200	78	253	28	7.6	0.24	3.7	1.9
120	200	91	215	31	8.2	0.26	4.0	2.0
360	200	85	196	32	8.5	0.27	4.2	2.1
360	200	78	225	30	8.1	0.26	4.0	2.0
360	200	71	230	30	8.0	0.25	3.9	2.0
High temperature								
1	336	243	194	32	8.5	0.27	4.2	2.1
3	341	247	213	31	8.2	0.26	4.1	2.0
10	350	232	231	30	8.0	0.25	3.9	2.0
10	341	234	203	31	8.4	0.27	4.1	2.1
9	347	247	207	32	8.4	0.27	4.1	2.1
20	352	239	204	31	8.3	0.26	4.1	2.0
41	351	213	206	31	8.3	0.26	4.1	2.0
120	350	220	252	23	6.0	0.19	3.0	1.5

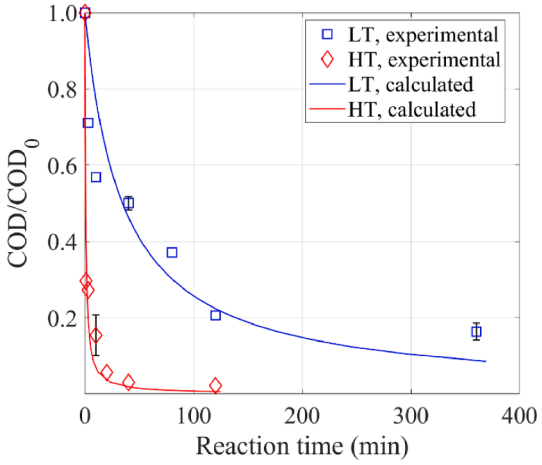

Fig. 5. Effect of temperature on COD reduction as a function of the reaction time. LT: Low temperature; HT: High temperature; Error bars: standard deviation for three repetitions.

continuous lines are calculated using the rate equation derived in Section 3.3.

As can be seen, the COD values decrease very rapidly for reaction times between 1 and 10 min. At HT, the slope of the curve reduces drastically after more than 90% of COD is converted. At LT, the slope of the curve reduces substantially for reaction times in the range of 120 to 360 min, even in the presence of unconverted species accounting for approximately 20% of the COD. This behavior is typically observed for the wet air oxidation of waste streams with high organic load, such as sewage sludge, for reaction temperatures around 240–250 °C [29]. A quantitative comparison of the COD decrease at a given reaction time of 10 min shows that approximately 80% of the COD is removed at HT (ca. 350 °C), while only 60% of the COD is removed at LT (ca. 200 °C). In addition, at HT conditions more than 93% COD reduction is achieved in 20 min, while the observed reduction of COD at LT does not exceed 85% even at very long times (i.e. 360 min). The COD reduction at HT reaches values up to 98%, which indicates that the oxidation reactions continue towards basically complete oxidation, albeit at a progressively reducing rate. The observed dramatic effect of the temperature increase on the reaction rate is in line with typical experimental findings in wet oxidation [12,13,30]. This effect can be explained by both a direct effect of temperature on the rate of the chemical reactions and by the increased oxygen solubility in the aqueous phase at the high-temperature high-pressure conditions of the HT runs. Indicatively, the solubility of oxygen in water is 3–4 g/kg at the LT conditions [31], whereas at the HT conditions it is one order of magnitude higher (i.e. 40 g/kg) [32].

3.3. Kinetic analysis

Considering the relative amount of oxygen and water at the conditions used in this work, the analysis of phase equilibrium data and phase envelopes for the system water-oxygen clearly indicates that the reaction is heterogeneous (gas–liquid) at LT conditions [31,33]. In addition, the available data suggest that the reaction is expected to be heterogeneous (gas–liquid) also at HT conditions [32]. Phase equilibrium data allowing to take into account the presence of the other species in the reaction system are not available. Overall, it was deemed reasonable to assume the reaction to be heterogeneous (gas–liquid) at both temperatures.

The kinetics of the oxidation reaction of organic pollutants is typically represented with respect to COD, which is used as a cumulative indicator of all oxidizable components dissolved in the aqueous solution [34–38]. The rate equation for the hydrothermal oxidation in the aqueous phase is generally expressed as a power-law equation [39]:

$$-r_{COD} = kCOD^{m}C_{O_2}^{n}$$

where $-r_{COD}$ expresses the mass of COD disappearing per unit time and volume of the reacting aqueous phase, COD is a mass-based concentration (mass of COD per unit volume of the reacting aqueous phase), and C_{O_2} is the mass-based concentration of oxygen in the reacting aqueous phase. The exponents m and n are the orders of the reaction with respect to COD and oxygen, respectively, and k is the rate constant. The concentration of oxygen in the reacting aqueous phase was assumed constant as a fair approximation, as the aqueous phase is assumed to be saturated with oxygen during the reaction. This is in line with approaches found in the literature, for aqueous phases kept under stirring at high rate and in the presence of a large excess of oxygen. These conditions lead to oxygen dissolution rates much higher than the oxygen consumption rate caused by the chemical reaction [35]. Under this assumption, the oxygen-term in the rate equation can be incorporated in the rate constant, thus giving a pseudo m-order reaction:

$$-r_{COD} = k' COD^{m}$$

The integral method of analysis was applied to the experimental data for m values of 0, 0.5, 1, 1.5, 2 and 3. The second order provided the best fit regarding the COD experimental data at both temperatures, with an R^2 of 0.89 and 0.96 for the low and high temperature, respectively. The order of the reaction with respect to COD in wet oxidation is typically observed between one and two [35,39]. By fixing the order of the reaction equal to two, the pseudo-rate constants (k') for the two temperatures were determined by applying a non-linear regression to the experimental data. The values were found to be 0.0011 $Lg^{-1}min^{-1}$ and 0.0725 $Lg^{-1}min^{-1}$ for the low and high temperature, respectively. The pseudo rate constant at the HT conditions is therefore 66 times higher than that at LT conditions. The calculated values are compared to the experimental data in Fig. 5 and demonstrate a good fit from a qualitative standpoint. On a quantitative basis, the root mean square error (RMSE) of the variable COD/COD_0 is 0.081 at low temperature and 0.089 at the high temperature.

3.4. Composition of the reaction products

The reaction products were free of HET, MEA and DTZ even at the shortest reaction times, which reflects their very fast degradation even at the lower reaction temperature (i.e. around 200 °C). A number of organic species were identified in the reaction products, including short-chain carboxylic acids (C1-C4) as well as pyridine, pyrazine and some of their alkyl- derivatives. Fig. 6 shows the trend of the TOC in the reaction products, together with the carbon-based yield (C-based yield) of the short-chain carboxylic acids and the pyridines-pyrazines, as a function of the reaction time. The C-based yield of a species is here defined as the mass of carbon of the species (or group of species) in the reaction product over the mass of organic carbon of the SUS fed to the reactor, which is estimated by means of the TOC_0. TIC data are not reported in Fig. 6, as the values are very low at all reaction times and appear to be rather insignificant. The complete experimental data is however reported in the Supplementary Information.

As can be seen, the TOC in the reaction products decreases with the reaction time, with a remarkable decrease occurring in the first minute of reaction at HT conditions, while the decrease is somewhat slower at LT conditions during the first 3 min. As the reaction progresses, TOC reductions down to 26% and 2% of the initial value are observed at LT and HT conditions, respectively. The TOC reduction in the aqueous reaction products is, with all probability, associated with the formation of carbon dioxide which is transferred to gas phase during the depressurization.

At LT conditions the vast majority of the organics which were identified and quantitated are carboxylic acids, with C-based yields in the range 6% to 13%, with the maximum observed at 120 min. In addition, a small amount of pyridines and pyrazines is observed only at long reactions times (i.e. 120 and 360 min) and with very low C-based yields (0.9%-1.2%). At HT both carboxylic acids and pyridines/pyrazines have similar C-based yields, in the range 0.4% to 6.9% and 0.2% to 7.6%, respectively. Both exhibit a maximum between 3 and 10 min, with values of 6.9% and 7.6%, respectively. These trends suggest that carboxylic acids are formed relatively fast both at LT and HT conditions, but while they are also relatively fast converted at HT conditions, they are slowly converted at LT conditions. The trends of pyridines/pyrazine may suggest a slower formation of these species. They are not stable though, as at HT conditions and long reaction times they are depleted. In terms of mass fractions in the aqueous reaction products, pyridines and pyrazines were found cumulatively in the range 0.012 to 0.88 g/kg, while the short-chain carboxylic acids were observed in the range 0.1 to 2.7 g/kg. It has to be noted that, especially at short reaction times, a large fraction of organic species is unidentified, when considering that HET, MEA and DTZ were not observed.

Fig. 7 shows the reduction of total nitrogen and the nitrogen-based yield (N-based yield) of NH_4^+ and NO_3^-, which are the two inorganic nitrogen-containing species identified in the reaction products, as well as the N-based yields of pyridine-pyrazine compounds. The N-based

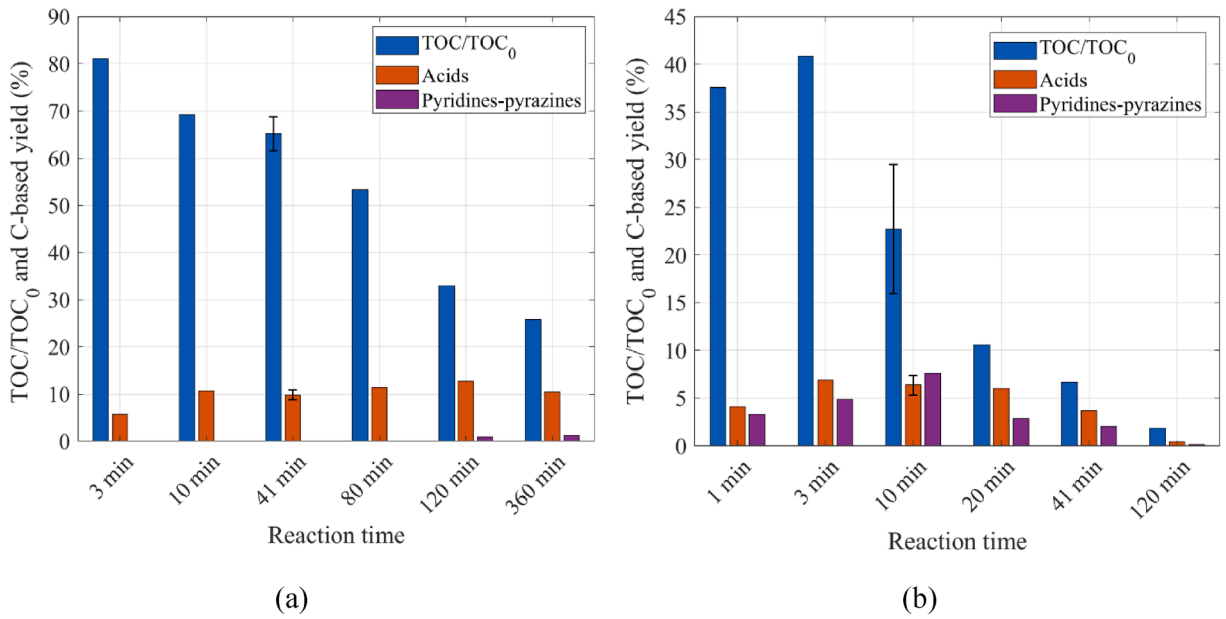

Fig. 6. TOC reduction (TOC/TOC_0) and carbon-based yield for short chain carboxylic acids, and pyridines-pyrazines as a function of the reaction time. (a) Low temperature and (b) high temperature experiments. Error bars are the standard deviation of triplicate experiments.

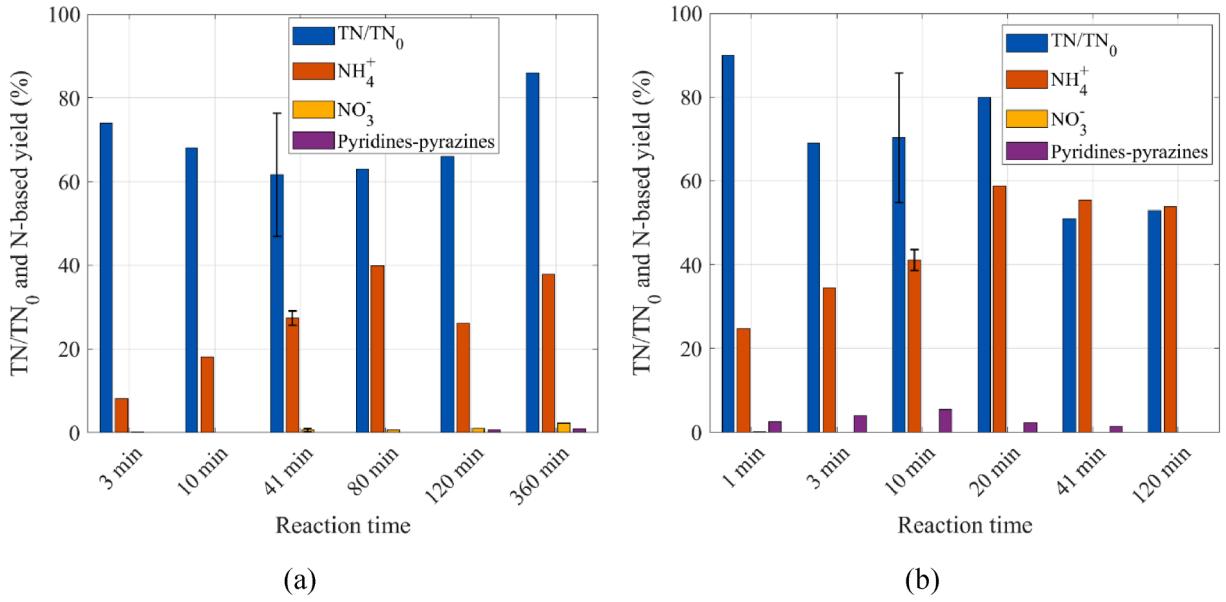

Fig. 7. Total nitrogen (TN/TN_0) and N-based yields of NH_4^+, NO_3^- and pyridine-pyrazine. (a) Low temperature and (b) high temperature experiments. Error bars are the standard deviation of triplicate experiments.

yield of a species is defined as the ratio of the mass of nitrogen of the species in the reaction product to the mass of total nitrogen in the reactor feed.

The presence of ammonium (or ammonia depending on the pH) and nitrate is typical in wet oxidation products of N-containing organic components, with ammonium often being a product of nitrogenous compounds that is refractory to oxidation [40]. More specifically, ammonia is reported as a wet oxidation product of MEA, although the literature refers to reactions below 100 °C [41,42]. In the present work, the pH of the reaction products ranged between 6.4 and 8.9, which implies that NH_4^+ is the predominant form in the NH_4^+/NH_3 equilibrium. The total nitrogen in the aqueous products is from 10% to 50% lower than the total nitrogen of the feed. Even though there is no clear trend of the total N over time and the SD on different product samples is rather high, the clear reduction compared to the feed suggests that some of the nitrogen is converted into nitrogen gas (N_2).

With regard to the individual N-containing species found in the aqueous products, the N-based yield of NH_4^+ increases over time in the first 80 min and 20 min at LT and HT conditions, respectively. The yield values reached at LT are around 40%, while they approach 60% at HT. Afterwards, the values appear to be approximately stable at LT and slowly decreasing at HT. NH_4^+ is rather stable in non-catalytic hydrothermal oxidation [40,43], although the slight reduction observed at HT and for reaction time 20–120 min indicates that it is slowly converted, even in the absence of a catalyst. Furthermore, Fig. 7b also shows that at HT conditions and long reaction times (i.e. 40 and 120 min), the nitrogen contained in NH_4^+ matches the residual total nitrogen in the aqueous products. In other words, NH_4^+ is the predominant N-containing

species that can be found in the aqueous phase at HT conditions and long reaction time, which is also in line with the progressive disappearance of pyridines/pyrazines at these conditions. With regard to NO_3^-, its N-based yield is very low at HT (i.e. 0.10–0.15%), while higher yields are observed at LT with an increasing trend up to approximately 2.3% after 360 min of reaction time. The cumulative N-based yield of pyridines and pyrazines is lower than 1% in the LT reaction products, while a maximum yield around 5.5% is obtained at HT conditions. Also in the case of nitrogen it can be seen that, especially at short reaction times, there is a large fraction of N-containing species in the aqueous products that is unidentified.

In Fig. 8 the total sulfur and the sulfur-based yield (S-based yield) of SO_4^{2-} are shown against the reaction time. The S-based yield of SO_4^{2-} increases relatively fast at both temperatures, reaching maximum values around 70% at LT and around 80% at HT, with the maximum reached after 10 min of reaction at LT and 20 min at HT. A very small decrease of sulfate is observed with the increase of the reaction time, which does not find any clear explanation. In addition, the observed reduction of the total sulfur in all samples cannot be explained as no sulfur-containing gaseous products are expected during hydrothermal oxidation [15].

However, the fact that the S-based yield of SO_4^{2-} in many cases exceeds the total sulfur indicates that the quantitation of sulfur by ICP suffers inaccuracies. On the whole, the fact that no other S-containing species are identified in the aqueous samples and the fact the SO_4^{2-} roughly matches all the sulfur in the aqueous phase, with the exception of the shortest reaction time at LT conditions, allows to state that SO_4^{2-} is the largely predominant S-containing product of the process.

The HPLC analysis with the use of analytical standards allowed the identification of some short-chain carboxylic acids in the reaction products. The only relevant ones, from a quantitative standpoint, were acetic, formic and succinic acids in the LT reaction products, while only acetic acid was found in considerable amount at HT conditions. Fig. 9 reports the carbon-based yield of the abovementioned acids individually.

At LT conditions, the maximum yields are seen from 4.6% (formic acid) to 7.5% (succinic acid), with the reaction times corresponding to the maxima increasing from 10 min (formic acid) to 120 min (succinic acid). With regard to HT conditions, the maximum yield of acetic acid appears as a large plateau for reaction times in the range of 3 to 20 min and yield values slightly below 6%. After 2 h of reaction at HT conditions, the yield of acetic acid is below 0.5%. The experimental observations pertaining to acetic acid aligns well with the literature, as acetic acid is one of the most common incomplete oxidation species identified in wastewaters subjected to hydrothermal oxidation at temperatures in the range 150 to 320 °C, while temperatures above 320 °C are reported to be appropriate for its conversion [18,37]. The organic components identified by SPME GC–MS in the reaction products were mainly pyridines and 1,2,4-trithiolane, with the latter also present in the feed. Even though it was not quantitated, its presence in the products suggests it is resistant to oxidation. Several peaks were observed in the chromatograms, with a few of them dominating the integrated chromatographic area. An example of chromatogram is shown in Fig. 10a, which is representative of all the reaction products since it includes all the major peaks. Most of the peaks that were identified were pyridine and some alkyl derivatives of pyridine, with 3-methyl pyridine being the most abundant. The SPME analysis enabled the development of the extraction and GC–MS analysis targeted to pyridines. Several pyridines were identified in the DEE extract, together with pyrazine and alkyl-pyrazines. An example of GC–MS chromatogram on the DEE extract is shown in Fig. 10b.

Fig. 11 shows the carbon-based yield of the pyridines and pyrazines individually, at HT conditions. The component that reaches the highest yield (i.e. 3.2%) is pyridine and is in addition the last of these components to be removed. Pyridine-ring components are found as oxidation intermediates of more complex components (e.g. quinoline), while pyridine itself is an intermediate of alkyl-pyridines (e.g. 2-methyl pyridine) [20,25]. The oxidation of pyridine itself has only been reported at supercritical water conditions, where it was oxidized to small carboxylic acids and ultimately to ammonia and CO_2 [44]. In the present work, while pyridine is almost completely oxidized between 40 and 120 min the ammonium yield between these reaction times remains very high, indicating that it is produced partly from the oxidation of pyridine.

4. Conclusion

A proof of concept of the hydrothermal oxidation of spent/unspent H_2S scavengers produced in offshore oil and gas units was provided. The process is appealing for treating this wastewater prior to the discharge into the sea, with the aim of substantially reducing the environmental impact of this practice. At high reaction severity (approximately 350 °C and 230 bar), the COD of the feed was observed to reduce more than

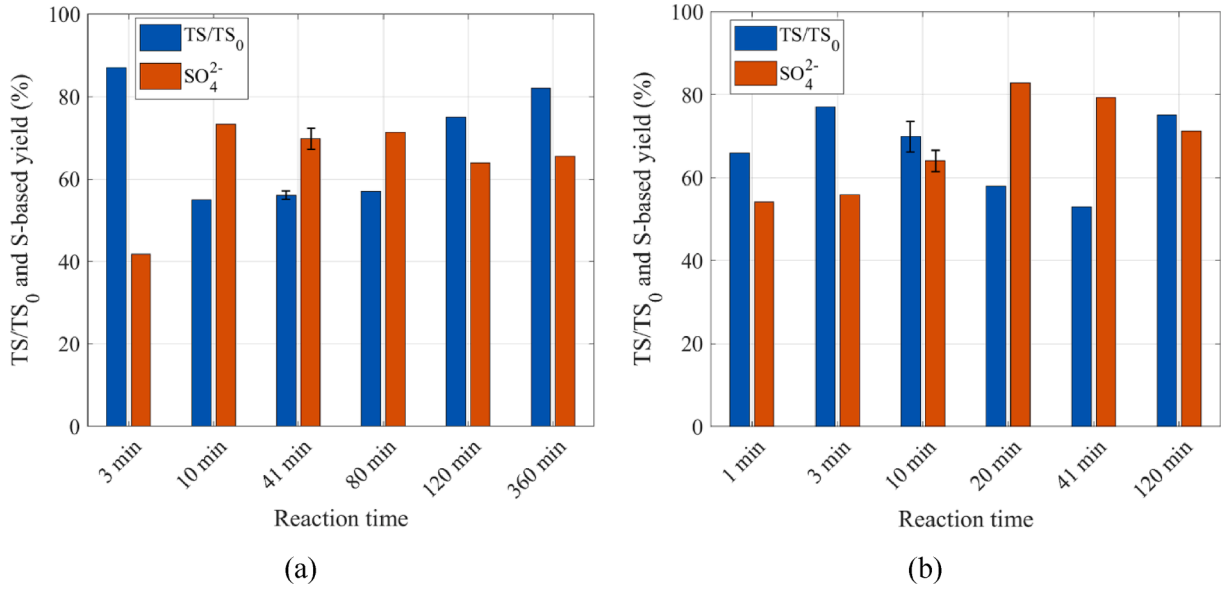

Fig. 8. Total sulfur (TS/TS_0) and S-based yields for SO_4^{2-}. (a) Low temperature and (b) high temperature experiments. Error bars are the standard deviation of triplicate experiments.

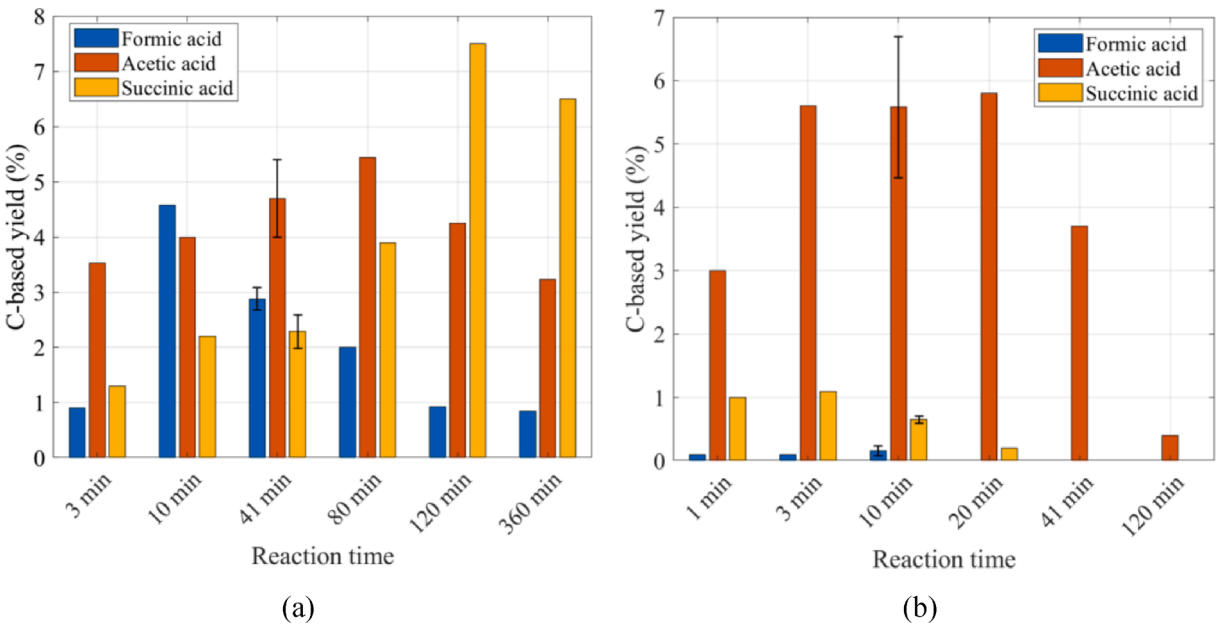

Fig. 9. Carbon-based yield for formic acid, acetic acid and succinic acid as a function of the reaction time. (a) Low temperature and (b) high temperature experiments. Error bars are the standard deviation of triplicate experiments.

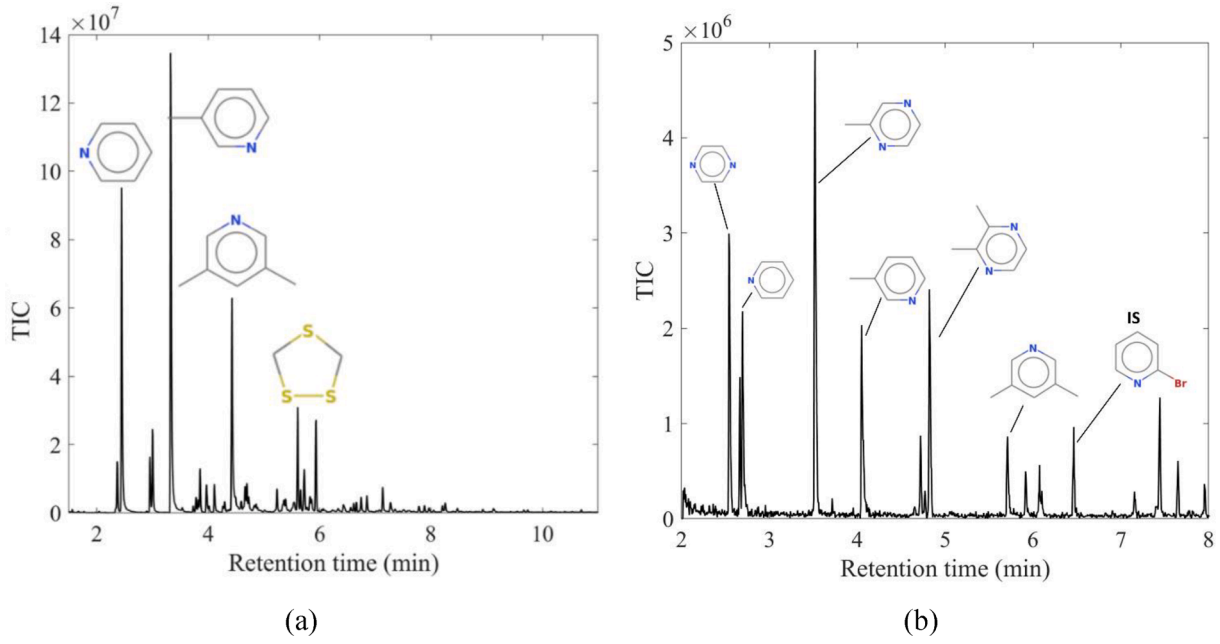

Fig. 10. (a) SPME GS-MS chromatogram for the oxidation at 346 °C and 10 min; (b) GC–MS of DEE extract for the oxidation at 341 °C and 3 min.

80% of the initial value (in the range 22 to 32 g/kg) with 10 min of reaction time, while the COD reduction reached 98% with 120 min of reaction time. The process is slower at low reaction severity (approximately 200 °C and 80 bar), with COD reduction of 43% in 10 min and 84% in 360 min. A simplified rate equation was validated on the experimental data, showing that the rate of reaction can be expressed as a fair approximation via a power-law equation of second order with respect to the COD.

The main species of the SUS feed, i.e. HET, DTZ and MEA, were fast converted, as they were not found even at the shortest reaction time under investigation (i.e. 1 min). The hydrothermal oxidation process was observed to lead to the mineralization of organic nitrogen to ammonium and, to a lower extent, to nitrate, as well as the mineralization of organic sulfur to sulfate.

Nitrogen gas and carbon dioxide are expected to be produced in large amount, as deduced by the decrease of the total nitrogen and the total carbon in the aqueous reacting phase. Intermediate oxidation products include carboxylic acids. This was proved by the quantitation of formic, acetic and succinic acid at low severity conditions, with the carbon-based yields of these species exhibiting maxima between 4% and 8% for reaction times in the range of 10 to 120 min. At high severity, acetic acid is the only acid observed in relatively large amount, showing a flat maximum of the carbon-based yield at almost 6% in the range 3 to 20 min. Other key intermediates identified and quantitated are pyridines and pyrazines. These species are observed to reach a maximum carbon-based yield between 0.9% and 3.2% for reaction times in the range 3 to

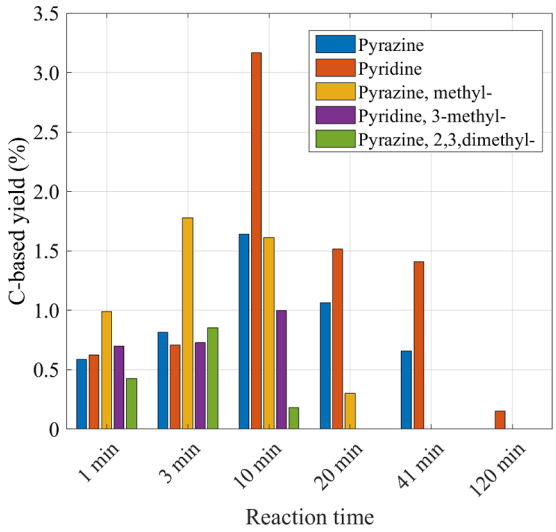

Fig. 11. Carbon-based yield of pyridines, pyrazines and their alkyl derivatives quantified by GC–MS as a function of the reaction time for the reaction products at high temperature.

10 min at high severity. On the other hand, at low severity these species are not observed for reaction times below 120 min.

A large fraction of C- and N-containing components was not identified, especially at short reaction times. Some uncertainties were also observed on the sulfur quantitation. Further identification of reaction intermediates is a possible topic for future investigations. In addition, since the target of the hydrothermal oxidation is ultimately to reduce the toxicity of the water discharge, the experimental observations open up for further research questions regarding the optimal operating conditions and reactor design for obtaining the largest toxicity reduction. These conditions do not necessarily stem from the largest COD reduction, as the development of toxic reaction intermediates, such as pyridine, may lead to larger toxicity reductions obtained for reaction conditions not coinciding with the minimum COD.

Declaration of Competing Interest

The authors declare that they have no known competing financial interests or personal relationships that could have appeared to influence the work reported in this paper.

Acknowledgments

The work was financially supported by The Danish Hydrocarbon Research and Technology Centre (DHRTC) as part of the work programme Produced Water Management. The authors would like to thank Jørgen Rentler Næumann (DHRTC, programme manager of the work programme Produced Water Management), Simon Ivar Andersen (DHRTC, research leader in Offshore Produced Water Management), Yanina D. Ivanova (DHRTC, production chemistry advisor) and Ole Andersen (DHRTC, surface engineer advisor) for the continuous and insightful technical discussions during the execution of this work. In addition, the authors would like to acknowledge the invaluable help of Linda Birkebæk Madsen (Aalborg University) for the execution of the total carbon, elemental and HPLC analysis and Dorte Spangsmark (Aalborg University) for the contribution in the development of the gas chromatographic and mass spectrometric analytical methodologies.

Appendix A. Supplementary data

Supplementary data to this article can be found online at https://doi.org/10.1016/j.cej.2021.131020.

References

[1] M.A. Kelland, Hydrogen Sulfide Scavengers, in: Production Chemicals for the Oil and Gas Industry, Second ed., CRC Press, 2014: pp. 353–368. https://doi.org/10.1201/b16648.
[2] G. Taylor, M. Smith-Gonzalez, J. Wylde, A.P. Oliveira, H2S scavenger development during the oil and gas industry search for an MEA triazine replacement in hydrogen sulfide mitigation and enhanced monitoring techniques employed during their evaluation, SPE-193536-MS, Proceedings - SPE International Conference on Oilfield Chemistry, Galveston, TX, USA, 2019.
[3] G.N. Taylor, P. Prince, R. Matherly, R. Ponnapati, R. Tompkins, P. Vaithilingam, Identification of the molecular species responsible for the initiation of amorphous dithiazine formation in laboratory studies of 1,3,5-tris (hydroxyethyl)-hexahydro-s-triazine as a hydrogen sulfide scavenger, Ind. Eng. Chem. Res. 51 (36) (2012) 11613–11617, https://doi.org/10.1021/ie301288t.
[4] G.N. Taylor, R. Matherly, Gas chromatographic-mass spectrometric analysis of chemically derivatized hexahydrotriazine-based hydrogen sulfide scavengers: Part II, Ind. Eng. Chem. Res. 49 (14) (2010) 6267–6269, https://doi.org/10.1021/ie1001247.
[5] J.J. Wylde, G.N. Taylor, K.S. Sorbie, W.N. Samaniego, Formation, chemical characterization and oxidative dissolution of amorphous polymeric dithiazine (apDTZ) during the use of the H2S scavenger monoethanolamine-triazine, Energy Fuels 34 (8) (2020) 9923–9931, https://doi.org/10.1021/acs.energyfuels.0c01402.
[6] Offshore Chemicals, OSPAR Commission. (2021). https://www.ospar.org/work-areas/oic/chemicals (accessed March 29, 2021).
[7] Monoethanolamine, ECHA. (2021). https://echa.europa.eu/substance-information/-/substanceinfo/100.208.078 (accessed March 29, 2021).
[8] M.D. Bermejo, F. Cantero, M.J. Cocero, Supercritical water oxidation of feeds with high ammonia concentrations. Pilot plant experimental results and modeling, Chem. Eng. J. 137 (3) (2008) 542–549, https://doi.org/10.1016/j.cej.2007.05.010.
[9] G. Brunner, Near and supercritical water. Part II: Oxidative processes, J. Supercrit. Fluids 47 (3) (2009) 382–390, https://doi.org/10.1016/j.supflu.2008.09.001.
[10] P.A. Marrone, Supercritical water oxidation - Current status of full-scale commercial activity for waste destruction, J. Supercrit. Fluids 79 (2013) 283–288, https://doi.org/10.1016/j.supflu.2012.12.020.
[11] H. Debellefontaine, J.N. Foussard, Wet air oxidation for the treatment of industrial wastes. Chemical aspects, reactor design and industrial applications in Europe, Waste Manageme. 20 (1) (2000) 15–25, https://doi.org/10.1016/S0956-053X(99)00306-2.
[12] A. Yousefifar, S. Baroutian, M.M. Farid, D.J. Gapes, B.R. Young, Fundamental mechanisms and reactions in non-catalytic subcritical hydrothermal processes: A review, Water Res. 123 (2017) 607–622, https://doi.org/10.1016/j.watres.2017.06.069.
[13] S.T. Kolaczkowski, P. Plucinski, F.J. Beltran, F.J. Rivas, D.B. McLurgh, Wet air oxidation: a review of process technologies and aspects in reactor design, Chem. Eng. J. 73 (2) (1999) 143–160, https://doi.org/10.1016/S1385-8947(99)00022-4.
[14] H.S. Joglekar, S.D. Samant, J.B. Joshi, Kinetics of wet air oxidation of phenol and substituted phenols, Water Res. 25 (2) (1991) 135–145, https://doi.org/10.1016/0043-1354(91)90022-I.
[15] S.K. Bhargava, J. Tardio, J. Prasad, K. Föger, D.B. Akolekar, S.C. Grocott, Wet oxidation and catalytic wet oxidation, Ind. Eng. Chem. Res. 45 (4) (2006) 1221–1258, https://doi.org/10.1021/ie051059n.
[16] C.E. Ellis, Wet air oxidation of refinery spent caustic, Environ. Prog. 17 (1) (1998) 28–30, https://doi.org/10.1002/ep.670170116.
[17] A. Prince-Pike, D.I. Wilson, S. Baroutian, J. Andrews, D.J. Gapes, A kinetic model of municipal sludge degradation during non-catalytic wet oxidation, Water Res. 87 (2015) 225–236, https://doi.org/10.1016/j.watres.2015.09.009.
[18] J.-N. Foussard, H. Debellefontaine, J. Besombes-Vailhé, Efficient elimination of organic liquid wastes: Wet air oxidation, J. Environ. Eng. 115 (2) (1989) 367–385, https://doi.org/10.1061/(ASCE)0733-9372(1989)115:2(367).
[19] A.M.T. Silva, R.M. Quinta-Ferreira, J. Levec, Catalytic and noncatalytic wet oxidation of formaldehyde. A novel kinetic model, Ind. Eng. Chem. Res. 42 (21) (2003) 5099–5108, https://doi.org/10.1021/ie030090r.
[20] A.B. Thomsen, Degradation of quinoline by wet oxidation - Kinetic aspects and reaction mechanisms, Water Res. 32 (1) (1998) 136–146, https://doi.org/10.1016/S0043-1354(97)00200-5.
[21] K.R. Arturi, M. Strandgaard, R.P. Nielsen, E.G. Søgaard, M. Maschietti, Hydrothermal liquefaction of lignin in near-critical water in a new batch reactor: Influence of phenol and temperature, J. Supercrit. Fluids 123 (2017) 28–39, https://doi.org/10.1016/j.supflu.2016.12.015.
[22] B. Raue, H.-J. Brauch, F.H. Frimmel, Determination of sulphate in natural waters by ICP/OES-comparative studies with ion chromatography, Fresenius J. Anal. Chem. 340 (6) (1991) 395–398, https://doi.org/10.1007/BF00321590.
[23] J. Prietzel, H. Cronauer, C. Strehl, Determination of dissolved total sulfur in aqueous extracts and seepage water of forest soils, Int. J. Environ. Anal. Chem. 64 (3) (1996) 193–203, https://doi.org/10.1080/03067319608028929.
[24] M. Colon, M. Iglesias, M. Hidalgo, J.L. Todolí, Sulfide and sulfate determination in water samples by means of hydrogen sulfide generation-inductively coupled plasma-atomic emission spectrometry, J. Anal. At. Spectrom. 23 (3) (2008) 416–418, https://doi.org/10.1039/B716302A.
[25] D.W. Allen, M.R. Clench, J. Morris, Investigation of the products of oxidation of methylpyridines under aqueous conditions by gas chromatography–mass spectrometry, Analyst 119 (5) (1994) 903–907, https://doi.org/10.1039/AN9941900903.

[26] M.H. Islam, V.M. Kaprielian, A. Bakó, M.E. Tertsch, R.P. Nielsen, M. Maschietti, Wet partial oxidation of guaiacol into carboxylic acids using hydrogen peroxide, Proceedings of the 26th European Biomass Conference and Exhibition (EUBCE 2018), 14-17 May 2018, Copenhagen, Denmark, pp. 1163–1168.
[27] S.A. Leont'eva, E.V. Podlesnova, A.A. Botin, E.I. Alatortsev, A.A. Dmitrieva, Determination of 1,2,4-trithiolane in oil and petroleum products by gas chromatography, J. Anal. Chem. 74 (12) (2019) 1209–1212, https://doi.org/10.1134/S1061934819120062.
[28] J.M. Bakke, J. Buhaug, J. Riha, Hydrolysis of 1,3,5-tris(2-hydroxyethyl)hexahydro-s-triazine and its reaction with H2S, Ind. Eng. Chem. Res. 40 (26) (2001) 6051–6054, https://doi.org/10.1021/ie010311y.
[29] E. Slavik, R. Galessi, A. Rapisardi, R. Salvetti, P. Bonzagni, G. Bertanza, L. Menoni, D. Orhon, S. Sözen, Wet oxidation as an advanced and sustainable technology for sludge treatment and management: Results from research activities and industrial-scale experiences, Drying Technol. 33 (11) (2015) 1309–1317, https://doi.org/10.1080/07373937.2015.1036282.
[30] V.S. Mishra, V.V. Mahajani, J.B. Joshi, Wet Air Oxidation, Ind. Eng. Chem. Res. 34 (1) (1995) 2–48, https://doi.org/10.1021/ie00040a001.
[31] E.F. Stephan, N.S. Hatfield, R.S. Peoples, H.A.H. Pray, The solubility of gases in water and in aqueous uranyl salt solutions at elevated temperatures and pressures, Report Nr. BMI-1067, Battelle Memorial Institute, Columbus, Ohio, 1956.
[32] M.L. Japas, E.U. Franck, High pressure phase equilibria and PVT-data of the water-oxygen system including water-air to 673 K and 250 MPa, Berichte Der Bunsengesellschaft Für Physikalische Chemie 89 (12) (1985) 1268–1275, https://doi.org/10.1002/bbpc.v89:1210.1002/bbpc.19850891206.
[33] F. Mangold, S. Pilz, S. Bjelić, F. Vogel, Equation of state and thermodynamic properties for mixtures of H_2O, O_2, N_2, and CO_2 from ambient up to 1000 K and 280 MPa, J. Supercrit. Fluids 153 (2019), 104476, https://doi.org/10.1016/j.supflu.2019.02.016.
[34] R.V. Shende, V.V. Mahajani, Kinetics of wet air oxidation of glyoxalic acid and oxalic acid, Ind. Eng. Chem. Res. 33 (12) (1994) 3125–3130, https://doi.org/10.1021/ie00036a030.
[35] H. Debellefontaine, M. Chakchouk, J.N. Foussard, D. Tissot, P. Striolo, Treatment of organic aqueous wastes: Wet air oxidation and wet peroxide oxidation®, Environ. Pollut. 92 (2) (1996) 155–164, https://doi.org/10.1016/0269-7491(95)00100-X.
[36] M.A. Imteaz, A. Shanableh, Kinetic model for the water oxidation method for treating wastewater sludges, Dev. Chem. Eng. Miner. Process. 12 (5-6) (2004) 515–530, https://doi.org/10.1002/apj.5500120507.
[37] R.V. Shende, V.V. Mahajani, Kinetics of wet oxidation of formic acid and acetic acid, Ind. Eng. Chem. Res. 36 (11) (1997) 4809–4814, https://doi.org/10.1021/ie970048u.
[38] J. Sánchez-Oneto, J.R. Portela, E. Nebot, E.J. Martínez-de-la-Ossa, Kinetics and mechanism of wet air oxidation of butyric acid, Ind. Eng. Chem. Res. 45 (12) (2006) 4117–4122, https://doi.org/10.1021/ie060103b.
[39] L. Li, P. Chen, E.F. Gloyna, Generalized kinetic model for wet oxidation of organic compounds, AIChE J. 37 (11) (1991) 1687–1697, https://doi.org/10.1002/aic.690371112.
[40] L. Oliviero, J. Barbier Jr., D. Duprez, Wet Air Oxidation of nitrogen-containing organic compounds and ammonia in aqueous media, Appl. Catal. B. 40 (2003) 163–184, https://doi.org/10.1016/S0926-3373(02)00158-3.
[41] S.J. Vevelstad, A. Grimstvedt, J. Elnan, E.F. da Silva, H.F. Svendsen, Oxidative degradation of 2-ethanolamine: The effect of oxygen concentration and temperature on product formation, Int. J. Greenhouse Gas Control 18 (2013) 88–100, https://doi.org/10.1016/j.ijggc.2013.06.008.
[42] A.J. Sexton, G.T. Rochelle, Reaction products from the oxidative degradation of monoethanolamine, Ind. Eng. Chem. Res. 50 (2) (2011) 667–673, https://doi.org/10.1021/ie901053s.
[43] D.K. Lee, J.S. Cho, W.L. Yoon, Catalytic wet oxidation of ammonia: Why is N_2 formed preferentially against NO_3? Chemosphere 61 (4) (2005) 573–578, https://doi.org/10.1016/j.chemosphere.2005.03.011.
[44] N. Crain, S. Tebbal, L. Li, E.F. Gloyna, Kinetics and reaction pathways of pyridine oxidation in supercritical water, Ind. Eng. Chem. Res. 32 (10) (1993) 2259–2268, https://doi.org/10.1021/ie00022a010.